Defraeye T., Lehmann V., Gross D., Holat C., Herremans E., Verboven P., Verlinden B., Nicolai B. (2013), Application of MRI for tissue characterisation of 'Braeburn' apple, *Postharvest Biology and Technology* 75, 96-105. http://dx.doi.org/10.1016/j.postharvbio.2012.08.009

Application of MRI for tissue characterisation of 'Braeburn' apple

Thijs Defraeye [a, *], Volker Lehmann [c], Dieter Gross [c], Carolin Holat [c], Els Herremans [a], Pieter Verboven [a], Bert E. Verlinden [b], Bart M. Nicolai [a,b]

[a] *MeBioS, Department of Biosystems, University of Leuven, Willem de Croylaan 42, 3001 Heverlee, Belgium*

[b] *VCBT, Flanders Centre of Postharvest Technology, Willem de Croylaan 42, 3001 Heverlee, Belgium*

[c] *Bruker Biospin GmbH, Silberstreifen 4, 76287 Rheinstetten, Germany*

Keywords

internal browning; MRI; apple; Braeburn; tissue; storage

Abstract

Magnetic resonance imaging (MRI) has become a well-established technique for non-destructive analysis of the internal (micro)structure of food, and the related heat, gas, water and solutes transport therein, which is of interest for food processing (e.g., drying), physical tissue damage assessment (e.g., bruising) for online sorting purposes or detection of internal defects (e.g., internal browning), amongst others. In contrast to previous MRI studies which predominantly analysed entire fruit, small samples (diameter ~ 10^{-2} m) of Braeburn apple were investigated in this study with high-field MRI, providing very local, high-resolution information, in order to identify the capability of MRI for detecting differences in fruit tissue types. The focus was on MRI for tissue characterisation with respect to inner and outer cortex tissue, fertilisation treatment, storage time and internal browning (IB). For this purpose, the proton density (PD), T_2 value and self diffusion coefficient (DC) were measured. No clear distinction could be made between samples with different fertilisation treatments. Differences in storage times could be observed from an increased PD for longer storage times. Inner tissue clearly showed an increased PD, T_2 value and DC, compared to the outer

[*] Corresponding author. Tel.: +32 (0)16 321618; fax: +32 (0)16 322966.
E-mail address: thijs.defraeye@biw.kuleuven.be

tissue. IB could be successfully detected, where the PD, T_2 value and the DC of the affected tissue were clearly higher than those of the healthy tissue, but a dependency of these parameters on the degree of tissue degradation was identified. Especially, the DC seemed to be an appropriate parameter regarding IB detection.

1. Introduction

Knowledge of the internal (micro)structure of fruit, and the related heat, gas, water and solutes transport therein, is of interest for many pre- and postharvest applications. Typical examples are analysis of tissue development during growth, physical tissue damage assessment (e.g., bruising), postharvest treatments to improve fruit quality and shelf life (e.g., heat treatments or storage conditions), food processing (e.g., drying or freezing) and online quality assessment for sorting purposes. Several experimental techniques have been applied for these purposes (Abbott et al., 1997; Falcone et al., 2006), such as X-ray computed tomography (Lammertyn et al., 2003a, 2003b; Verboven et al., 2008; Musse et al., 2010), near infrared spectroscopy (NIR, Clark et al., 2003; Nicolai et al., 2007) or magnetic resonance imaging (MRI, Clark et al., 1997; Hills and Clark, 2003; Lammertyn et al., 2003a, 2003b). MRI has become a well-established technique for the analysis of fruit and other food due to the following features (Clark et al., 1997): (1) MRI is non-intrusive, hence non-destructive, which allows monitoring of intact samples (e.g., fruit) over time; (2) MRI is very suitable for fruit, due to their high water content and the sensitivity of MRI to quality parameters affecting the fruit (e.g., browning); (3) 3-D high spatial resolution information on the internal fruit structure is available (typical slice thickness ~ 100-1000 μm; resolution in 2-D slice ~ 10-50 μm; voxel volume ~ 10 nL); (4) Different parameters related to the microstructure, water distribution and its mobility can be measured (proton density PD, T_1 and T_2 value, self diffusion coefficient), which often provide complementary information; (5) Different substances (e.g., water, oil, sugar) can be distinguished.

For apple fruit in particular, MRI has already been applied to analyse: (1) changes within the tissue during ripening and storage (Letal et al., 2003); (2) internal quality defects such as voids, worm damage or bruising and their variation over time (Chen et al., 1989; McCarthy et al., 1995; Zion et al., 1995); (3) the 3-D

vascular structure (MacFall and Johnson, 1994); (4) the microporosity (air volume) of apple (Musse et al., 2010); (5) temporal degradation of apples by watercore (Marlow and Loescher, 1984; Wang et al., 1988; Cho et al., 2008), internal browning (Clark and Burmeister, 1999; Gonzalez et al., 2001; Chayaprasert and Stroshine, 2005; Cho et al., 2008) or mealiness (Barreiro et al., 2000; Marigheto et al., 2008); (6) drying of apple (McCarthy et al., 1991; Hills and Remigereau, 1997; Nguyen et al., 2006); (7) transport properties and chemical composition of apples (Verstreken et al., 1997; Keener et al., 1999); (8) water compartmentation in apple tissue (Snarr and Van As, 1992). Note that some of these applications used low-field magnetic resonance sensors (Snarr and Van As, 1992; Hills and Remigereau, 1997; Keener et al., 1999; Chayaprasert and Stroshine, 2005; Cho et al., 2008; Marigheto et al., 2008).

A large amount of valuable research has thus already been performed on MRI of apples (and fruit in general) but some aspects can still be explored more in detail. Most of the aforementioned studies applied MRI from the perspective of its non-destructive nature, where MRI is argued to be particularly suitable for monitoring fruit quality over time and detection of internal defects but also for online quality assessment (e.g., on a conveyor belt). Although there is still a long way to go before online MRI can be applied in practice, i.e. cost-effective and at a realistic throughput, research towards this particular application is ongoing (Clark et al., 1997; Chayaprasert and Stroshine, 2005; Cho et al., 2008). Thereby, nearly all studies considered entire apples (except Verstreken et al., 1997; Marigheto et al., 2008), by which the entire range of substructures of the apple fruit (vascular bundles, pits, voids near the core, inner and outer cortex tissue) is comprised in the MRI image. Performing MRI at a higher resolution (smaller field of view) could provide more detailed information by a more local assessment of MRI parameters (e.g., T_2 value). In addition, MRI parameters (e.g., PD or T_2 value) of several of these substructures are often lumped together in the analysis, for example by not differentiating between inner and outer cortex tissue, which induces biasing of the tissue structure variability over the fruit. Also, tissue characteristics which could be detectable with MRI, such as the change of tissue structure with storage time, can become "invisible" in this way. Furthermore, most studies looked at changes in proton density and T_2 (or T_1) values to assess quality, but not at the self diffusion coefficient of water.

This study aims at addressing the aforementioned issues on MRI for apple fruit, as not all of them have been considered in detail in previous studies, in order to contribute to the existing knowledge base of MRI research on fruit tissue. These issues mainly concern evaluating which features of fruit tissue can be distinguished additionally with MRI, for example the change of tissue structure with storage time. Such distinctions are of use for several of the applications mentioned in the second paragraph of this section. Note that such characterisations of specific tissues with MRI (e.g. fertilisation) are not all directly of commercial interest, but they can be contribute in future studies to the general understanding of the physiology and metabolism of fruit, which in time can lead to better preharvest and postharvest storage strategies. Small samples are investigated with high-field MRI , providing very local, high-resolution information, in order to obtain more detailed information, compared to when considering an entire fruit. The focus is on tissue characterisation, where inner and outer cortex tissue, different fertilisation types, different storage times and different storage conditions, i.e., for internal browning detection, are considered. For this purpose, the proton density, T_2 value and self diffusion coefficient are measured.

2. Materials and methods

2.1. Apple fruit

Apples (*Malus* × *domestica* Borkh) cv. Braeburn were used for this study. Two cultivation treatments were applied: optimal fertilisation (treated with 30 kg/hectare calcium nitrate, 20 kg/hectare phosphorus, no potassium) and suboptimal fertilisation (treated with 30 kg/hectare ammonium nitrate, 20 kg/hectare phosphorus, 80 kg/hectare potassium). The fertilisation was applied on March 24th 2010. The apples were harvested on October 27th 2010, which was considered to be the optimal harvest date for long-term commercial storage for Belgium, as determined by the Flanders Centre of Postharvest Technology (VCBT). Afterwards, each type of apple was stored under two types of controlled atmosphere (CA): browning inducing storage conditions (1% O_2, 5% CO_2, 1°C), starting on October 29th, and optimal storage conditions

(2.5% O_2, 0.7% CO_2, 1°C), starting on November 16th (3 week delay of CA to prevent browning). These pre- and postharvest treatments resulted in four batches of apples, which were labelled GG, BB, GB and BG. The first letter indicates the storage conditions and the second indicates the fertilisation type, where G is used for optimal (good) conditions and B for suboptimal (bad) conditions. Two MRI measurements campaigns were performed, namely one month after harvesting (November 23rd - 25th) and four months after harvesting (March 1st - March 4th). Note that none of the apples used during the first campaign were stored in CA. Instead, after harvest they were all stored for one month at 1°C under normal air conditions, by which these apples only differed with respect to fertilisation treatment. Consequently, for the first measurement campaign, only the fertilisation type is indicated in the sample name, i.e., 0G and 0B. As Braeburn is quite susceptible for internal browning (IB), some apples analysed during the second measurement campaign, the BB type in particular, showed IB.

2.2. MRI: system, image acquisition and postprocessing

Proton (^{1}H) magnetic resonance images of apple samples were made in a AVIII 500WB nuclear magnetic resonance (NMR) spectrometer (Bruker Biospin, Germany), equipped with a high-field 11.7 T superconducting magnet, a Micro2.5 gradient system (2.5 G/cm/A gradient sensitivity) and a 1H 500 MHz MicWB40 probe with a quadrature birdcage coil of 30 mm inner diameter.

2-D MRI multi-spin echo measurements (16 echoes) were performed on specific slices within the sample. Due to the finite thickness of these slices (~ 1 mm), information on a thin 3-D volume was actually obtained. The resulting MRI signal intensity (S) is a function of experimental parameters (echo time T_E and repetition time T_R) and sample-specific parameters (proton density PD, T_1 and T_2 relaxation values) (e.g., Gonzalez et al., 2001):

$$S = c \cdot PD\left[1 - e^{-T_R/T_1}\right]e^{-T_E/T_2} \quad (1)$$

where c is a constant, characteristic for the NMR spectrometer. Since MRI measurements with different T_E were performed (multi-spin echo), contrast was provided regarding T_2 values in particular (transverse (spin-

spin) relaxation time), i.e., T_2 weighted images. The signal intensity and the T_2 value distribution over the individual slices were determined by regression analysis on the MRI signal by fitting a two-parameter exponential recovery curve of the signal intensity on the 16 corresponding signal intensity points (echoes) per slice. In principle, the PD is directly proportional to the MRI signal intensity (Clark et al., 1997; Gonzalez et al., 2001), as also assumed in this study. However, this requires that the signal intensity (S) has been corrected for relaxation times since without such a correction, changes in signal intensity (internal variation within sample, or change at a specific location in the sample over time) could be due to changes of PD but also of relaxation times (see Eq.(1), Gonzalez et al., 2001). Such a correction was accounted for in this study for the T_2 value, as the signal intensity was determined by evaluating the fitted two-parameter exponential recovery curve to $T_E = 0$. A correction for the T_1 value was not performed as its influence was considered less critical due to the rather large T_R value. Note that the proton density cannot be directly related to the moisture content without proper calibration (i.e. scaling). Furthermore, the spatially-resolved self diffusion coefficients of water (DC) were also measured for a few samples by a diffusion-weighted spin echo method. The postprocessing was done with Paravision 5.1 software (developed by Bruker Biospin). The relevant experimental characteristics are presented in Table 1.

The PD indicates the amount of protons within the slice volume. Due to the abundance of water in fruit (moisture content of apple ≈ 80%), the PD is mainly related to the presence of water, but also solutes (sugars or proteins) contribute. In some cases, other properties, e.g., T_2 relaxation, can provide better contrast than the PD. Volumes with spins of shorter T_2 relaxation time appear with lower signal intensities in the NMR images. T_2 relaxation is suggested to be caused by fast proton exchange between water and solutes and by diffusion of water protons through internally-generated magnetic field gradients (Hills and Duce, 1990; Duce et al., 1992; Clark et al., 1997). Such magnetic field gradients are caused by magnetic susceptibility differences in inhomogeneous tissue in a magnetic field, e.g., at the interface between air- and liquid-filled pores. These gradients thus depend on air porosity, pore size distribution and the pore shape (surface to volume ratio of pores). The T_2 values thus reflect to some extent the structure and the mobility of the protons, thus of water inside of the tissue. This could be useful to distinguish free water and water bound to/in

between cell walls. The self diffusion coefficient of water relates to the mobility of the water molecules with respect to their Brownian motion. It is thus a measure of the diffusion/movement of the substance in itself. Apart from the PD, T_2 value and DC, which were selected for this study based on previous experiments on fruit, the T_1 value can also be determined from T_1 weighted images. These NMR parameters (PD, T_1 and T_2 values, DC) are commonly reported in MRI studies (Clark et al., 1997).

From the MRI data, statistics were calculated of each slice by considering a circular region of interest (ROI) which included nearly the entire sample (cylindrical, see section 2.3). Only the edge zones were not included since the tissue cells here were damaged to some extent from the extraction with the cork borer (see section 2.3). Following statistics were calculated for the PD, the T_2 value and the DC: average and standard deviation.

In addition to the spin echo method, the gradient echo method (GE) was also evaluated at the high magnetic field of 11.7 T. The GE method however did not provide good contrast for Braeburn apples with internal browning disorder, but it provided good contrast for apples with watercore disorder (results not shown). This could be related to the fact that the GE method at high magnetic fields was very sensitive to local susceptibility changes caused by water/air interfaces which reduced the image intensities almost to zero intensity. Therefore, the GE method could not distinguish well the cell-void-cell structure, but it was actually more suitable for watercore detection, due to the more homogeneous gel-like structure in watercore tissue. For low-field MRI with specific settings, the GE method was however found to provide better contrast than the spin echo method to detect bruising (McCarthy et al., 1995).

2.3. Tissue characterisation experiments

Apple tissues with different characteristics (e.g. IB) were analysed by slicing small cylindrical samples (diameter 25 mm, height ± 5 mm) from a cylindrical apple core (diameter 25 mm), which was extracted with a cork borer along the apple equator, as shown in Figure 1. Samples were taken from the inner cortex tissue

(close to the core) and from the outer cortex tissue (close to the skin). For each measurement, four samples were stacked on one another in a cylindrical test tube, which was mounted in the coil of the NMR spectrometer (inner diameter 30 mm, Figure 2a). MRI was performed on a slice in the centre of each sample (Figure 2b). An overview of the measured samples is presented in Table 2. Note that within a specific sample, distinct heterogeneity could be found for samples which contained IB or vascular bundles, as indicated in section 3.

2.4. Statistical analysis of fertiliser, storage and cortex tissue effects

An analysis of variance (ANOVA) was carried out using SAS software, version 9.2 (SAS Institute Inc., Cary, NC, USA) to determine significant effects of fertiliser treatment, CA storage conditions and storage time as well as to test differences between inner and outer tissue on the statistics derived from the MRI data.

3. Results and discussion

The influence of fertilisation type, storage time (one month - four months), tissue type (inner or outer) and IB (related to storage conditions) on the MRI data is analysed to see to what extent these features can be distinguished by means of MRI. Both the PD and the T_2 value are evaluated for this purpose, and for a few samples also the DC. Note that the units of PD are arbitrarily. The mean values of the MRI-data statistics over the ROI (average and standard deviation of the MRI pixel distributions) of the different apple tissue sample types (see Table 2) are presented in Figures 3-4. Error bars indicate the 95% confidence intervals, based on the standard deviation on the mean values (of each ROI) considering all relevant samples, assuming a normal distribution. In Figure 5, the corresponding relative frequency distributions of the PD and T_2 value of these samples are presented. For samples which showed visual IB (inner tissue of BB and BG), the affected tissue will have an impact on the PD and T_2 value statistics. Therefore, these samples are discussed separately in section 3.4 during the analysis of IB, but they are included in Figures 3-5 for completeness. Furthermore, it has to be acknowledged that the magnitude of the T_2 value depends to some extent on the strength of the magnetic field, due to changing field inhomogeneities at interfaces of tissues with different

magnetic susceptibilities (Musse et al., 2010). In addition, T_2 values can also vary for different species and pre- and postharvest treatments, as shown below. Comparison with T_2 values from previous research is thereby not entirely justified and relative comparison of these values within a specific batch of fruit is more appropriate. Note that, in addition to the aforementioned statistics, ANOVA was also performed (section 2.4) to support the analysis of Figures 3-4.

Relatively large confidence intervals (thus standard deviations on the mean values) are found for some sample types in Figures 3-4 indicating a large intersample heterogeneity. Note that also a relatively small amount of samples was measured (Table 2), where an evaluation of more samples would provide more reliable statistics. Such an extensive measurement campaign and the subsequent data analysis would be very time consuming, and is not practically feasible for most applications of MRI in food engineering: MRI studies are usually developing/applying MRI for detection of internal defects, online damage detection, e.g., on a conveyor belt, or for process engineering (e.g., drying processes). Here, MRI should thus provide fast but accurate information of the internal quality of food, namely for each individual specimen. From this perspective, this study aims at investigating which characteristics can clearly be distinguished with MRI, thus taking into account some intersample variability.

3.1. Fertilisation

The influence of the fertilisation type is analysed from Figures 3-4 by comparing: (1) the 0G with the 0B samples (one month storage); (2) the GG/BG with the BB/GB samples (four months storage). No significant differences between 0G and 0B samples can be noticed for the PD (average and standard deviation) of both inner and outer tissue: the mean value of one type usually falls well in between the confidence interval of the other one. A trend towards higher average T_2 value is indicated by the 0B samples. When comparing the GG/BG with the BB/GB samples however, higher T_2 values for apples with suboptimal fertilisation are not confirmed. With ANOVA, the influence of the fertilisation type is also found to be not distinctive. The used

fertilisation treatment cannot clearly be distinguished by the MRI measurements performed in this study. This is not surprising since the influence of fertilisation is expected to have an impact on the storage life and shelf life, rather than on the water compartmentation in apple fruit and the related cell microstructure.

3.2. Storage time

The influence of storage time is analysed by comparing samples with one month storage and those with four months storage in Figures 3-5. Regarding the outer tissue, a distinction between both storage periods can be noticed, with higher values of the PD and T_2 after four months storage. For the inner tissue, a trend to systematically higher PD is also found, but the T_2 value is, however, lower. The increase in PD with storage time for inner and outer tissue is rather counter-intuitive since fruit lose moisture during storage (albeit small), so they should contain less water. However, this moisture loss is to some extent accompanied with the development of Braeburn browning disorder, which could induce a partial destruction of the cellular integrity prior to the formation of larger cavities (Lammertyn et al., 2003a). This will change the water distribution and compartmentation in the tissue, which could lead to the higher PD values: e.g., the inner tissue samples of BB and BG, showing clear IB thus a partially destroyed cell integrity, have the largest PD. These microstructural changes will also alter the water mobility, but only a slight trend towards higher T_2 values for the outer tissue can be noticed. From ANOVA, the storage conditions are found to be clearly distinctive for the average PD. Note that generally, the amount of solutes remains quasi constant during storage, which thereby will not be a reason for an increased PD. The PD standard deviation after four months storage is larger for outer tissue but especially for inner tissue. For this parameter, ANOVA also confirmed storage to be distinctive.

3.3. Inner and outer tissue

The influence of the tissue type (inner or outer cortex tissue) is analysed by comparing the samples for each type of apple (0G, 0B, GG, BB, GB, BG) separately, with respect to the tissue type, in Figures 3-4 and by

comparing the distributions of inner and outer tissue in Figure 5. As mentioned, samples which showed IB (inner tissue) are not discussed in this section, but note that their data are included in the analysis in this section. Typical PD, T_2 and DC maps of inner and outer tissue are shown in Figure 6 for a GG type apple sample. The more heterogeneous nature of the inner tissue is clearly visible. Vascular bundles (visible in the outer tissue) appear brighter (for PD), in agreement with findings of Zion et al. (1995).

For each apple type (e.g., GG), the average PD and T_2 values of the inner tissue are higher than those of the outer tissue. This indicates and confirms the lower porosity, higher moisture content and the larger pore size of the inner tissue of apple, and thus also the higher water mobility (Schotsmans et al., 2004; Verboven et al., 2008; Mendoza et al., 2010). Furthermore, a higher T_2 standard deviation of the inner tissue is found (Figure 4), compared to the outer tissue (mean value for all samples: inner tissue: 9.0, outer tissue: 7.0). These higher values of the standard deviation could indicate the increased heterogeneity of the inner tissue's microstructure. These findings are confirmed by ANOVA: the difference between inner and outer tissue for the T_2 value is found to be distinctive for the average value and the standard deviation.

No clear trend is visible between the PD standard deviation of inner and outer tissue of each apple type, and their overall value is approximately similar (mean value for all samples: inner tissue: 116.4, outer tissue: 115.7). From ANOVA, a distinctive difference between inner and outer tissue for the PD is found for the average value, but not for the standard deviation, confirming the aforementioned findings.

For a few samples (of GG and BB), self diffusion coefficient (DC) measurements were performed (see Table 2). The statistics are presented in Figure 7 for both inner and outer tissue. The corresponding relative frequency distribution is presented in Figure 8. The DC of the inner tissue shows much higher values than that of the outer tissue (both for healthy, i.e., GG, and affected tissue, i.e., BB), indicating the higher water mobility here, which is probably related to the larger cell sizes of the inner tissue (Schotsmans et al., 2004). Regarding standard deviation, no clear trends can be observed apart from the rather high values (and spread) for samples showing IB. ANOVA only indicated distinctive differences for the average DC value of both

tissues. For comparison purposes, the obtained DCs are presented in Figure 9 together with those from previous MRI experiments. The results of the present study lie quite centralised within this range. Note that a large spread on the MRI data is found regarding apple cultivars.

In conclusion, the PD, T_2 value and DC are found to be all suitable MRI parameters for differentiation between inner or outer tissue types. The T_2 value (and its statistics) seems to reflect the heterogeneity (higher standard deviation) of the inner tissue better, compared to the PD. Based on the few DC measurements that were performed however, the DC seems to allow the most clear distinction between both types (i.e., the largest differences of average values). These findings regarding tissue types are partially in contrast with previous research by Musse et al. (2010). Although they argued that the overall heterogeneity within the apple, namely the major morphological features (e.g., vascular bundles), could be distinguished by T_2 maps, they indicated that different parts of the apple cortex could not clearly be distinguished by multi-spin echo images, which was shown to be possible in this study. Note that Keener et al. (1999) was able to distinguish between tissues of different apple cultivars, based on the T_2 value and DC, using low-field MRI.

3.4. Internal browning

The influence of IB, related to the storage conditions (CA), is analysed by comparing the samples of inner tissue with visual IB (BB and BG, browning inducing CA storage) and without visual IB (GG and GB, optimal CA storage). The statistics of the PD, the T_2 value and the DC of these samples are presented in Figures 3-4 and Figure 7 and their relative frequency distribution is given in Figures 5 and 8. Note that the samples showing IB are not entirely affected, by which the influence of IB is biased to some extent by the unaffected tissue, as indicated below. A typical BB sample is shown in Figure 10, together with the PD, T_2 value and the DC. In Figure 11, the average values of the PD, T_2 value and DC are reported for the entire sample of Figure 10 but also locally for ROI's of healthy and affected tissue separately. The corresponding PD, T_2 value and DC frequency distribution of these ROI's of the BB sample are reported in Figure 12. Note that the mean values for all GG and BB samples are also included in Figure 11.

When considering the entire sample (inner tissue), the PD and the DC of the affected samples (BB and BG) are higher than that of the healthy samples (GG and GB) but both generally fall in between each other's confidence interval. From ANOVA, only the PD was found to be distinctive with respect to storage conditions (IB). These overall sample data are however biased to some extent by the local unaffected tissue for BB and BG samples, by which a local assessment of these MRI parameters is more suitable, e.g., as indicated in Figure 12. From Figures 10-12, the (local) PD, T_2 value and the DC of the affected tissue are clearly higher than those of the healthy tissue. The presence of these two tissue types is also noticeable in the distribution of the entire sample in Figure 12: for the PD distribution and to a lesser extent for the T_2 value distribution, the affected tissue results in a tail to the right, i.e., higher skewness, but for the DC, even two distinct peaks appear (bimodal distribution). This could explain the higher (overall) PD and DC which are found for BB type samples, compared to GG type samples (Figure 11). The biasing of the influence of IB by the unaffected tissue with respect to the PD, T_2 value and DC of the entire sample is also obvious from Figure 11.

From the PD, T_2 value and DC maps of Figure 10, a region with lower values is found in the centre of the IB, which is in contrast to the higher values that are generally found for affected tissue (as discussed in the previous paragraph). This could be due to the partial destruction or degradation of the cellular structure, by which water migrates to other regions in the fruit (and by which the diamagnetic susceptibility variations decrease), leading to less water availability and mobility, and consequently the formation and presence of cavities. Similar observations were made by McCarthy et al. (1995), which found lower T_2 values for bruised regions in apple fruit. Furthermore, it is remarkable that for the T_2 value, the demarcation between healthy and affected tissue is characterised by an increased T_2 value, i.e., with higher values than in the IB region. From these observations, different stages of IB seem to exhibit a different sensitivity to each of these MRI parameters, related to different free water contents. A similar hypothesis, made by Lammertyn et al. (2003b) for pear tissue, could explain the observed differences in MRI parameters within the affected tissue: initially, the cell membranes in the tissue are affected and cells lose their integrity, resulting locally in a higher free

water content (high PD, T_2 value and DC in the affected tissue in Figure 10). Consequently, this water diffuses away and evaporates, leading to drier, brown tissue with cavities (lower PD, T_2 value and DC in the centre of the affected tissue in Figure 10). In the present study, a clear dependency of the different MRI parameters on the degree of tissue degradation was identified for apple tissue.

In agreement with the present study, an increased signal intensity (thus PD) for IB areas was found by Clark and Burmeister (1999) for Braeburn apple. According to Gonzalez et al. (2001), however, this increased intensity could be related to the fact that no correction for relaxation times was applied for the signal intensity (S), which is assumed to be directly proportional to the PD (e.g., Clark et al., 1997; Gonzalez et al., 2001). Without such a correction, changes in signal intensity could be due to changes of PD but also of relaxation times (see Eq.(1), see section 2.2). Based on this correction, Gonzalez et al. (2001) found a lower PD for IB for Fuji apples. In this study, such a correction was applied for the T_2 value but not for the T_1 value, as this was considered less critical (as discussed in section 2.2). Future studies will investigate the necessity of a correction for the T_1 value more in detail. However, as mentioned in the previous paragraph, both higher and lower PD can be found in affected tissue, depending on the rate of cellular degradation and the rate of diffusion and evaporation of water out of the material. For the same reason, Lammertyn et al. (2003b) also found lower PD intensities for affected tissue for pears, whereas Wang and Wang (1989) found higher intensities.

As in the present study, Gonzalez et al. (2001) found higher T_2 values for dark brown areas. Gonzalez et al. (2001) argued that the T_2 value provides the best contrast, compared to the T_1 value and the PD. From this study (Figures 11-12), the DC however seems to be an even more appropriate parameter for IB detection. In general, regarding the detection of IB with MRI, the present study agrees with previous studies (e.g., Clark and Burmeister, 1999; Gonzalez et al., 2001): IB detection with MRI provides similar results as visual detection.

Note that these previous studies looked at an apple fruit with severe IB, namely where nearly the entire core (inner) tissue was affected. Here, the healthy tissue with which comparison was made, was nearly always outer tissue. As significant differences were found between inner and outer tissue for the MRI parameters (section 3.3), comparison between inner IB tissue and outer healthy tissue is not entirely justified as two parameters simultaneously affect the MRI results: internal browning but also tissue type, which could have an opposite effect. Healthy and IB tissue, both from the inner cortex, should actually be compared, which was done in the present study.

Low-field MRI studies on IB (Keener et al., 1999; Chayaprasert and Stroshine, 2005; Cho et al., 2008), usually applied the Carr-Purcell-Meiboom-Gill (CPMG) pulse sequence technique for T_2 value evaluation. Often the resulting signal was fitted with an exponential equation, with one or more exponential terms. One or more parameters in this equation were then associated to T_2 relaxation. A lower T_2 has been found for IB (Keener et al., 1999; Chayaprasert and Stroshine, 2005), in contrast to the present study and other studies not using the CPMG pulse sequence. Using a three-term exponential model, Cho et al. (2008) found a more complex dependency of the T_2-related parameters on IB. Furthermore, Keener et al. (1999) found no effect of IB on the self diffusion coefficient of water, in contrast to the present study.

4. Conclusions

In this study, high-field MRI was used for tissue characterisation of apples of the Braeburn variety. In contrast to most previous studies, small samples were considered instead of an entire apple, providing very local, high-resolution information. The aim of such tissue characterisation was to identify which differences in tissue types could be clearly distinguished with MRI, i.e., with respect to inner and outer cortex tissue, fertilisation treatment, storage time (i.e., duration of CA storage) and internal browning (IB, related to storage conditions). The quantities chosen for this analysis were the proton density (PD), the T_2 value and the self diffusion coefficient of water (DC). No clear distinction could be made between samples with different fertilisation treatments. Differences in storage times could be observed from an increased PD for longer

storage times. Inner tissue clearly showed an increased PD, T_2 value and DC, compared to outer tissue. IB could be successfully detected, where the PD, T_2 value and the DC of the affected tissue were clearly higher than those of the healthy tissue but a dependency of these parameters on the degree of tissue degradation was identified. Especially the DC seemed to be an appropriate parameter regarding IB detection. Such tissue characterisation, i.e., the topic of the present study, is an important step towards the commercial use of MRI for non-destructive quality control, e.g., for IB or mealiness detection.

Acknowledgements

Thijs Defraeye is a postdoctoral fellow of the Research Foundation – Flanders (FWO) and acknowledges its support. This publication has been produced with the financial support of the European Union (project FP7-226783 - InsideFood), the Research Foundation – Flanders (project G.0603.08), and the KU Leuven (project OT 08/023). The opinions expressed in this document do by no means reflect the official opinion of the sponsors.

References

Abbott, J.A., Lu, R., Upchurch, B.L., Stroshine, R.L., 1997. Technologies for non-destructive quality evaluation of fruits and vegetables. Hortic. Rev. 20, 1-120.

Barreiro, P., Ortiz, C., Ruiz-Altisent, M., Ruiz-Cabello, J., Fernández-Valle, M.E., Recasens, I., Asensio, M., 2000. Mealiness assessment in apples and peaches using MRI techniques. Magn. Reson. Imaging 18, 1175-1181.

Chayaprasert, W., Stroshine, R., 2005. Rapid sensing of internal browning in whole apples using a low-cost, low-field proton magnetic resonance sensor. Postharvest Biol. Tec. 36, 291-301.

Chen, P., McCarthy, M.J., Kauten, R., 1989. NMR for internal quality evaluation of fruits and vegetables. T. ASAE 32, 1747-1753.

Cho, B.-K., Chayaprasert, W., Stroshine, R.L., 2008. Effects of internal browning and watercore on low field (5.4 MHz) proton magnetic resonance measurements of T_2 values of whole apples. Postharvest Biol. Tec. 47, 81-89.

Clark, C.J., Burmeister, D.M., 1999. Magnetic resonance imaging of browning development in 'Braeburn' apple during controlled-atmosphere storage under high CO_2. HortScience 34, 915-919.

Clark, C.J., Hockings, P.D., Joyce, D.C., Mazucco, R.A., 1997. Application of magnetic resonance imaging to pre- and post-harvest studies of fruits and vegetables. Postharvest Biol. Tec. 11, 1-21.

Clark, C.J., McGlone, V.A., Jordan, R.B, 2003. Detection of Brownheart in 'Braeburn' apple by transmission NIR spectroscopy. Postharvest Biol. Tec. 28, 87-96.

Duce, S.L., Carpenter, T.A., Hall, L.D., Hills, B.P., 1992. An investigation of the origins of contrast in NMR spin echo images of plant tissue. Magn. Reson. Imaging 10, 289-297.

Falcone, P.M., Baiano, A., Conte, A., Mancini, L., Tromba, G., Zanini, F., Del Nobile, M.A., 2006. Imaging techniques for the study of food microstructure: A review. Adv. Food Nutr. Res. 51, 205-263.

Gonzalez, J.J., Valle, R.C., Bobroff, S., Biasi, W.V., Mitcham, E.J., McCarthy, M.J., 2001. Detection and monitoring of internal browning development in 'Fuji' apples using MRI. Postharvest Biol. Tec. 22, 179-188.

Hills, B.P., Clark, C.J., 2003. Quality Assessment of Horticultural Products by NMR. Ann. R. NMR S. 50, 75-120.

Hills, B.P., Duce, S.L., 1990. The influence of chemical and diffusive exchange on water proton transverse relaxation in plant tissues. Magn. Reson. Imaging 8, 321-331.

Hills, B.P., Remigereau, B., 1997. NMR studies of changes in subcellular water compartmentation in parenchyma apple tissue during drying and freezing. Int. J. Food Sci. Technol. 32, 51-61.

Keener, K.M., Stroshine, R.L., Nyenhuis, J.A., 1999. Evaluation of low field (5.40 MHz) proton magnetic resonance measurements of D_w and T_2 as methods of nondestructive quality evaluation of apples. J. Am. Soc. Hortic. Sci. 124, 289-295.

Lammertyn, J., Dresselaers, T., Van Hecke, P., Jancsók, P., Wevers, M., Nicolai, B.M., 2003a. MRI and X-ray CT study of spatial distribution of core breakdown in 'Conference' pears. Magn. Reson. Imaging 21, 805-815.

455 Lammertyn, J., Dresselaers, T., Van Hecke, P., Jancsók, P., Wevers, M., Nicolai, B., 2003b. Analysis of the
456 time course of core breakdown in 'Conference' pears by means of MRI and X-ray CT. Postharvest Biol.
457 Tec. 29, 19-28.
458 Létal, J., Jirák, D., Suderlová, L., Hájek, M., 2003. MRI 'texture' analysis of MR images of apples during
459 ripening and storage. Lebensm. Wiss. Technol. 36, 719-727.
460 MacFall, J.S., Johnson, G.A., 1994. The architecture of plant vasculature and transport as seen with magnetic
461 resonance microscopy. Can. J. Bot. 72, 1561-1573.
462 Marigheto, N., Venturi, L., Hills, B., 2008. Two-dimensional NMR relaxation studies of apple quality.
463 Postharvest Biol. Tec. 48, 331-340.
464 Marlow, G.C., Loescher, W.H., 1984. Watercore, in: Janick, J. (Ed.), Horticultural Reviews - Volume 6.
465 John Wiley & Sons Inc., New Jersey, USA, pp. 189-251.
466 McCarthy, M.J., Perez, E., Ozilgen, M., 1991. Model for transient moisture profiles of a drying apple slab
467 using the data obtained with magnetic resonance imaging. Biotechnol. Prog. 7, 540-543.
468 McCarthy, M.J., Zion, B., Chen, P., Ablett, S., Darke, A.H., Lillford, P.J., 1995. Diamagnetic susceptibility
469 changes in apple tissue after bruising. J. Sci. Food Agr. 67, 13-20.
470 Mendoza, F., Verboven, P., Ho, Q.T., Kerckhofs, G., Wevers, M., Nicolai, B., 2010, Multifractal properties
471 of pore-size distribution in apple tissue using X-ray imaging. J. Food Eng. 99, 206-215.
472 Musse, M., De Guio, F., Quellec, S., Cambert, M., Challois, S., Davenel, A., 2010. Quantification of
473 microporosity in fruit by MRI at various magnetic fields: comparison with X-ray microtomography.
474 Magn. Reson. Imaging 28, 1525-1534.
475 Nguyen, T., Dresselaers, T., Verboven, P., D'hallewin, G., Culeddu, N., Van Hecke, P., Nicolai, B., 2006.
476 Finite element modelling and MRI validation of 3D transient water profiles in pears during postharvest
477 storage. J. Sci. Food Agric. 86, 745-756.
478 Nicolai, B.M., Beullens, K., Bobelyn, E., Peirs, A., Saeys, W., Theron, K.I., Lammertyn, J., 2007.
479 Nondestructive measurement of fruit and vegetable quality by means of NIR spectroscopy: A review.
480 Postharvest Biol. Tec. 46, 99-118.

Schotsmans, W., Verlinden, B.E., Lammertyn, J., Nicolai, B., 2004. The relationship between gas transport properties and the histology of apple. J. Sci. Food Agr. 84, 1131-1140.

Snarr, J.E.M., Van As, H., 1992. Probing water compartments and membrane permeability in plant cells by ^{1}H NMR relaxation measurements. Biophys. J. 63, 1654-1658.

Verstreken, E., Van Hecke, P., Scheerlinck, N., De Baerdemaeker, J., Nicolaï, B., 1998. Parameter estimation for moisture transport in apples with the aid of NMR imaging. Magn. Reson. Chem. 36, 196-204.

Veraverbeke, E.A., Verboven, P., Scheerlinck, N., Hoang, M.L., Nicolai, B.M., 2003. Determination of the diffusion coefficient of tissue, cuticle, cutin and wax of apple. J. Food Eng. 58, 285-294.

Verboven, P., Kerckhofs, G., Mebatsion, H.K., Ho, Q.T., Temst, K., Wevers, M., Cloetens, P., Nicolai, B.M., 2008. Three-dimensional gas exchange pathways in pome fruit characterized by synchrotron x-ray computed tomography. Plant Physiol. 147, 518-527.

Wang, C.Y., Wang, P.C., 1989. Nondestructive detection of core breakdown in 'Bartlett' pears with nuclear magnetic resonance imaging. Hort. Sci. 24, 106-109.

Wang, S.Y., Wang, P.C., Faust, M., 1988. Non-destructive detection of watercore in apple with nuclear magnetic resonance imaging. Sci. Hortic. 25, 227-334.

Zion, B., Chen., P., McCarthy, M.J., 1995. Detection of bruises in magnetic resonance images of apples. Comput. Electron. Agr. 13, 289-299.

500 **Figures**

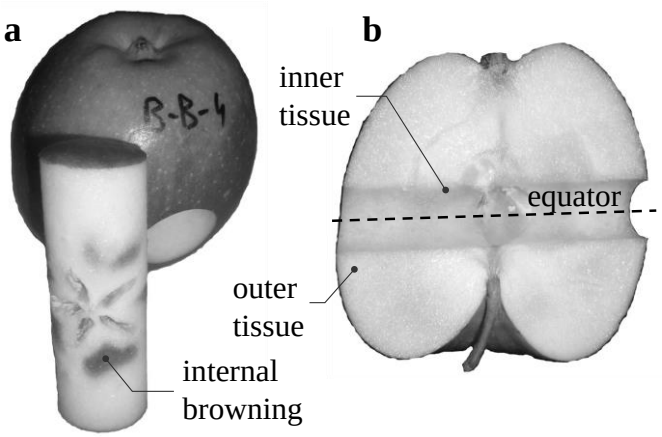

501

502 **Figure 1. Cylindrical apple core, taken along equator (with cork borer), from which cylindrical**

503 **samples were cut: (a) overview; (b) section through apple.**

504

505

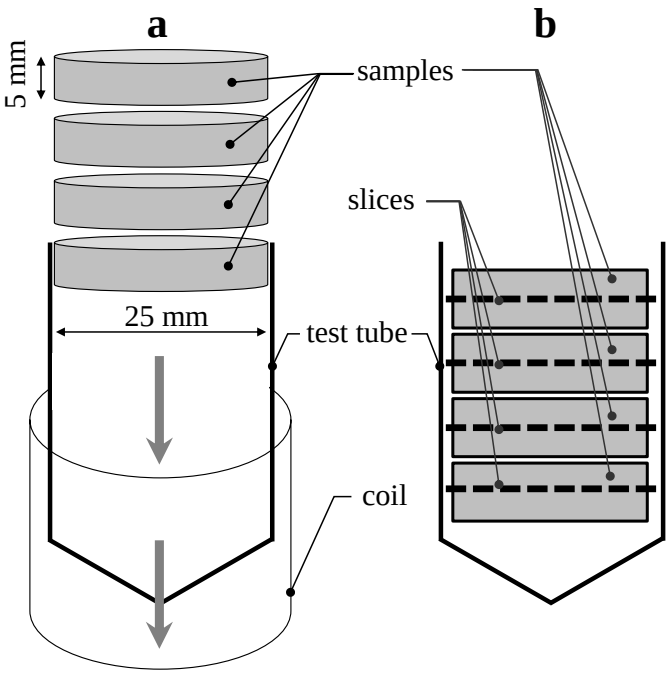

506

507 **Figure 2. (a) Mounting of four cylindrical apple samples by means of a test tube in the coil of the NMR**

508 **spectrometer; (b) Side view of test tube with four samples where transverse slices are indicated.**

509

510

511

512

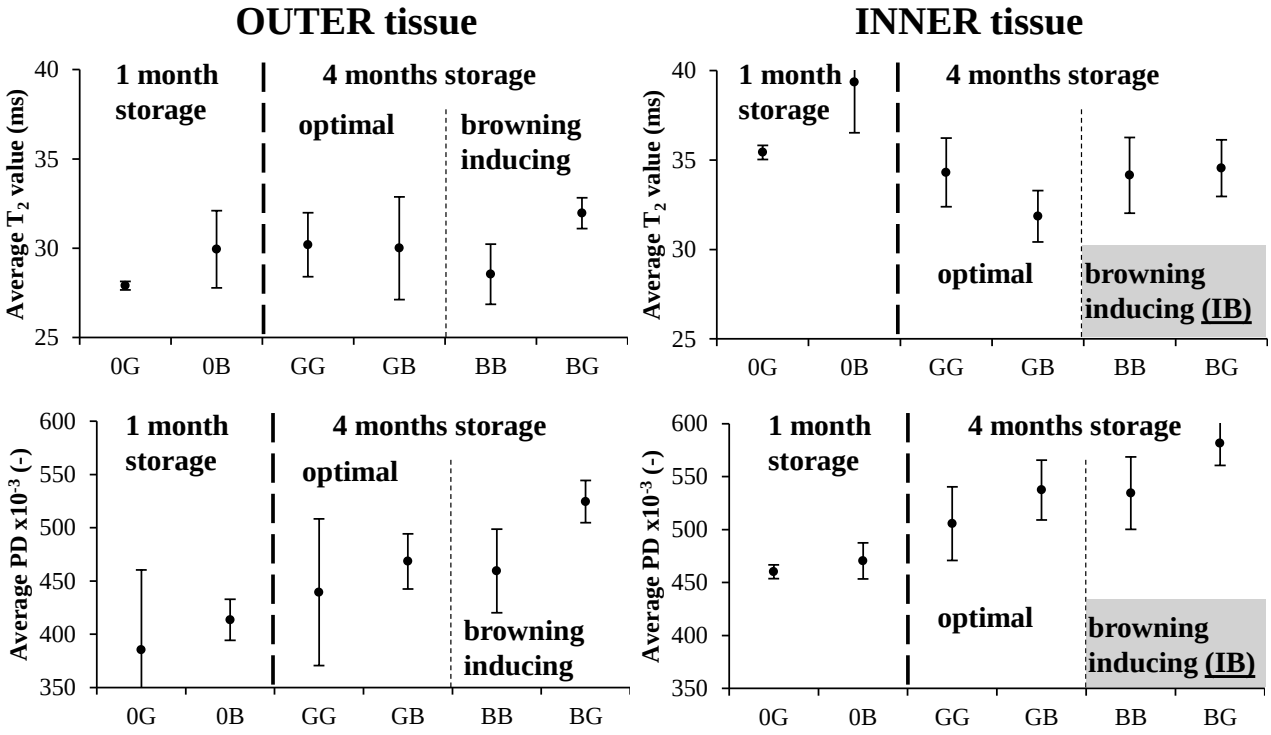

Figure 3. Average T_2 value and proton density (of the ROI) of apple samples taken from both the inner and outer tissue for apples with different fertilisation types and storage conditions. The mean value of all considered samples (see Table 2) and the 95% confidence intervals for this mean value are shown (indicated with error bars).

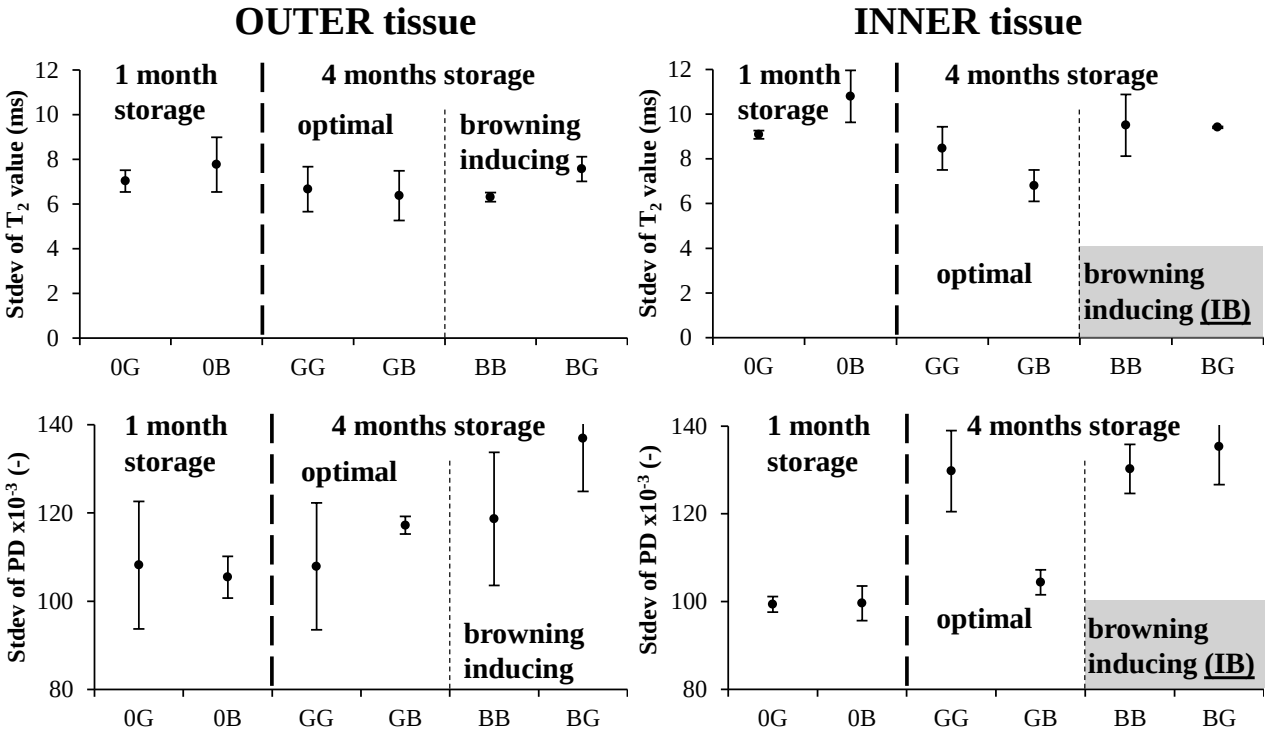

519

520 **Figure 4. Standard deviation (Stdev) of T_2 value and proton density (of the ROI) of apple samples**
521 **taken from both the inner and outer tissue for apples with different fertilisation types and storage**
522 **conditions. The mean value (of the standard deviation) of all considered samples (see Table 2) and the**
523 **95% confidence intervals for this mean value are shown (indicated with error bars).**

524

525

526

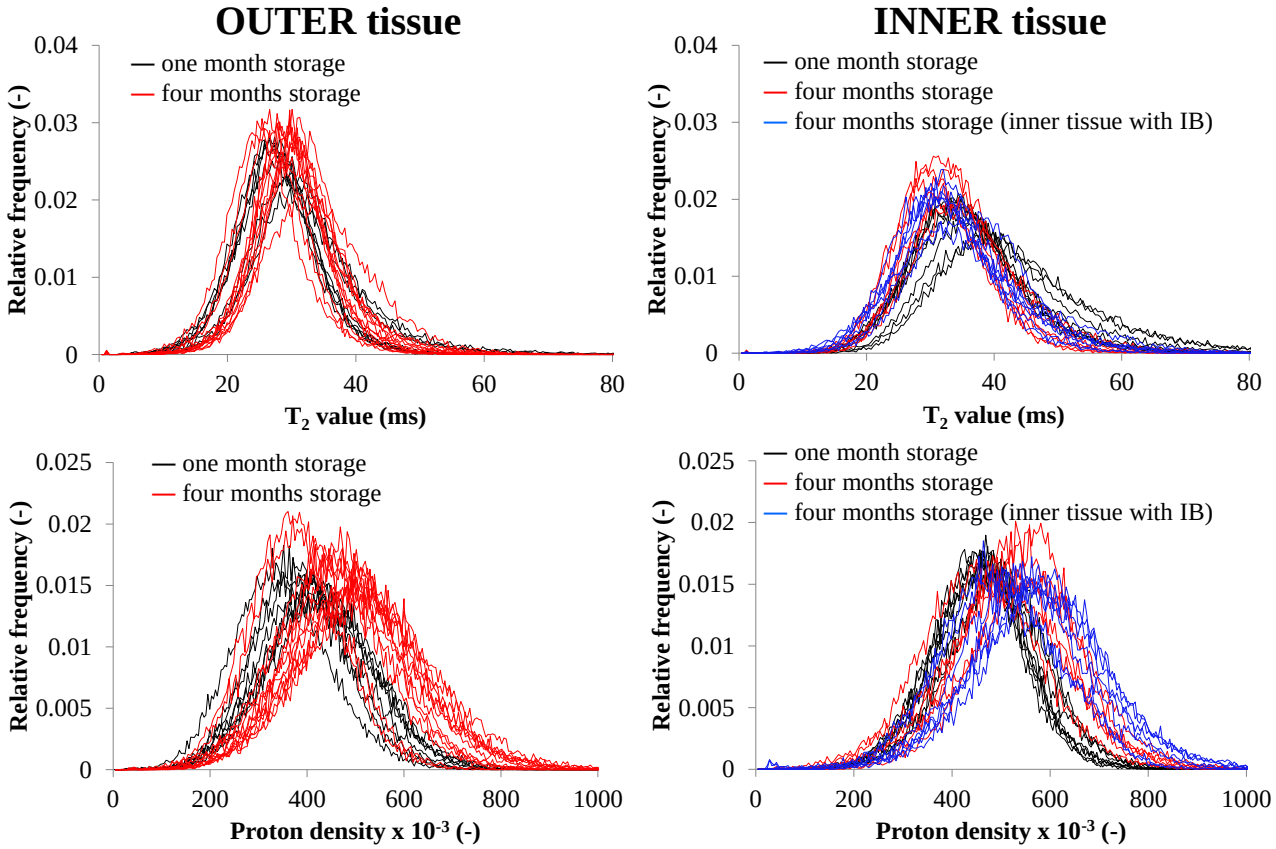
OUTER tissue
INNER tissue
one month storage
four months storage
four months storage (inner tissue with IB)
Relative frequency (-)
T2 value (ms)
Proton density x 10-3 (-)

527

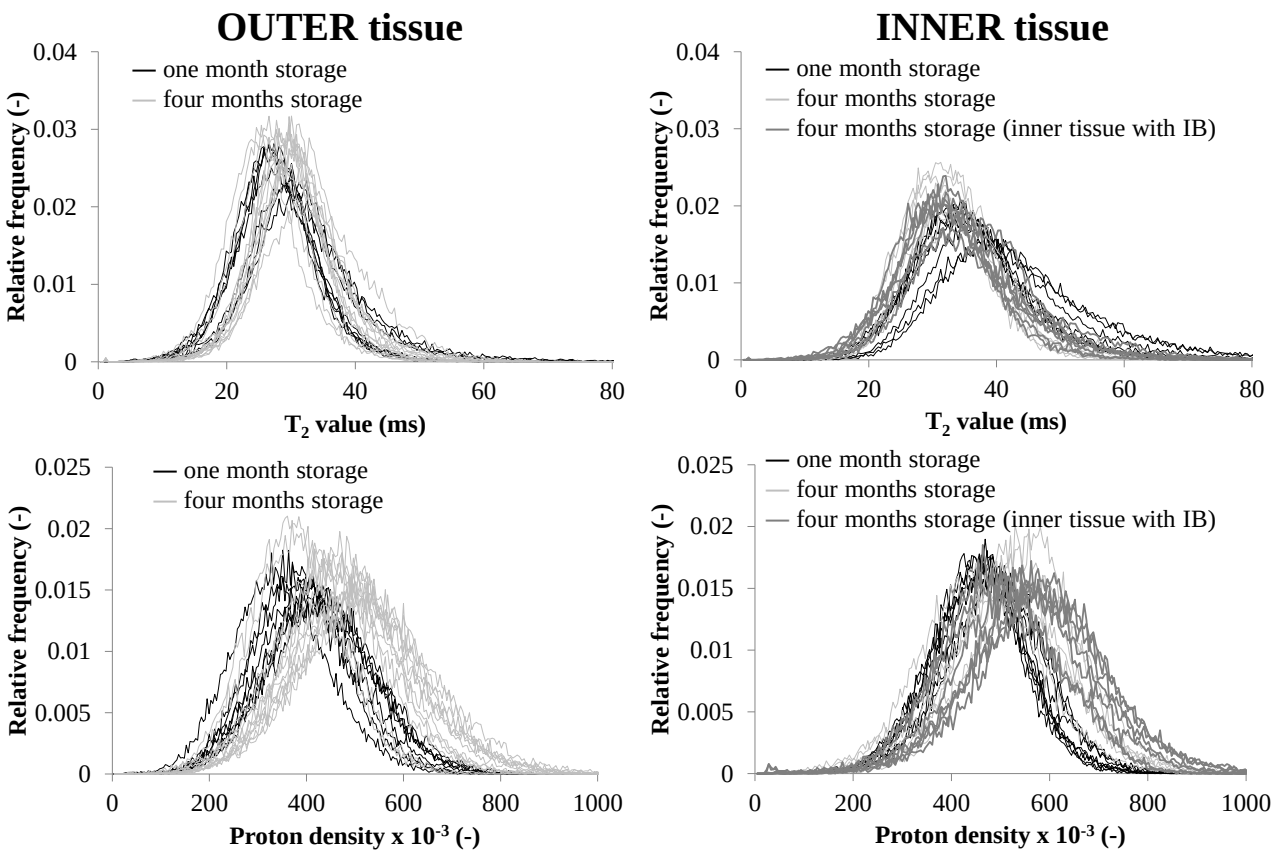
OUTER tissue
INNER tissue
one month storage
four months storage
four months storage (inner tissue with IB)
Relative frequency (-)
T2 value (ms)
Proton density x 10-3 (-)

528

529 **Figure 5. Relative frequency distribution of T_2 value and proton density (of the ROI) for inner and**
530 **outer tissue: Distinction between apples after one month (black lines) and four months storage (red**
531 **and blue lines). Samples with visual internal browning are represented by blue lines.**

532

533

534

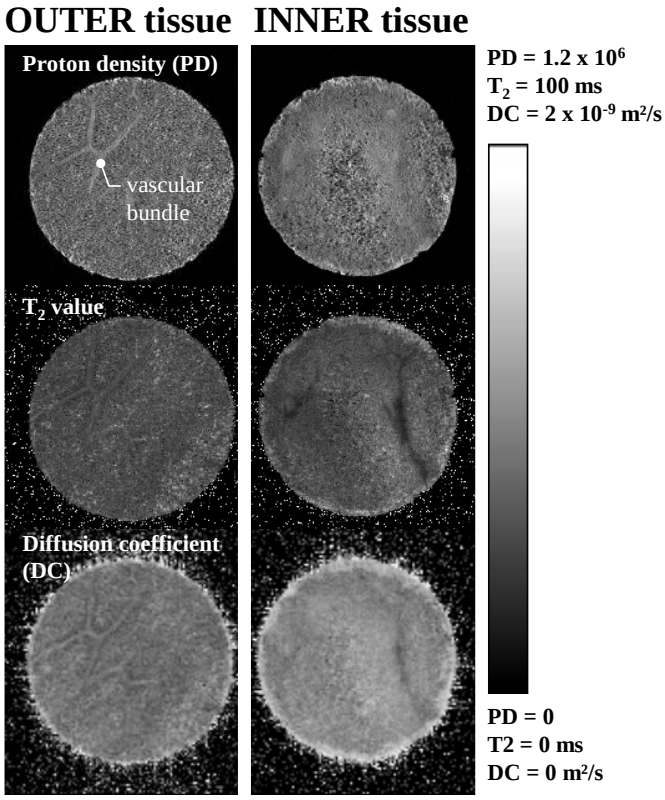

Figure 6. Proton density, T_2 value and diffusion coefficient maps of a typical GG apple sample for inner and outer tissue.

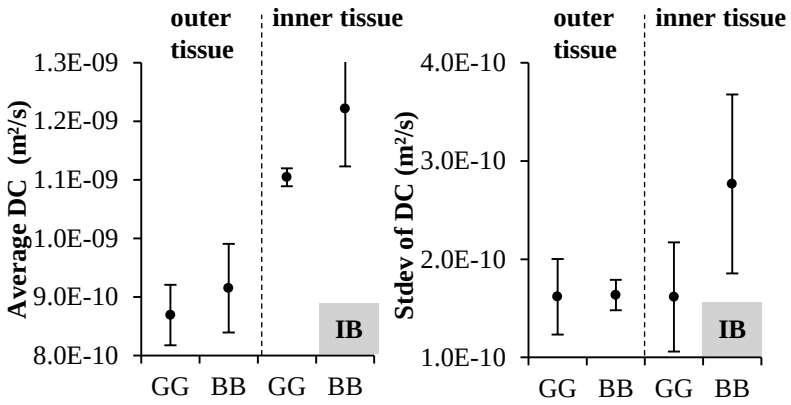

Figure 7. Average and standard deviation (Stdev, of the ROI) of the diffusion coefficient (DC) of apple samples taken from both the inner and outer tissue for apples with different fertilisation types and storage conditions (types BB and GG). The mean value (of each parameter) of all considered samples (see Table 2) and the 95% confidence intervals for this mean value are shown (indicated with error bars).

548

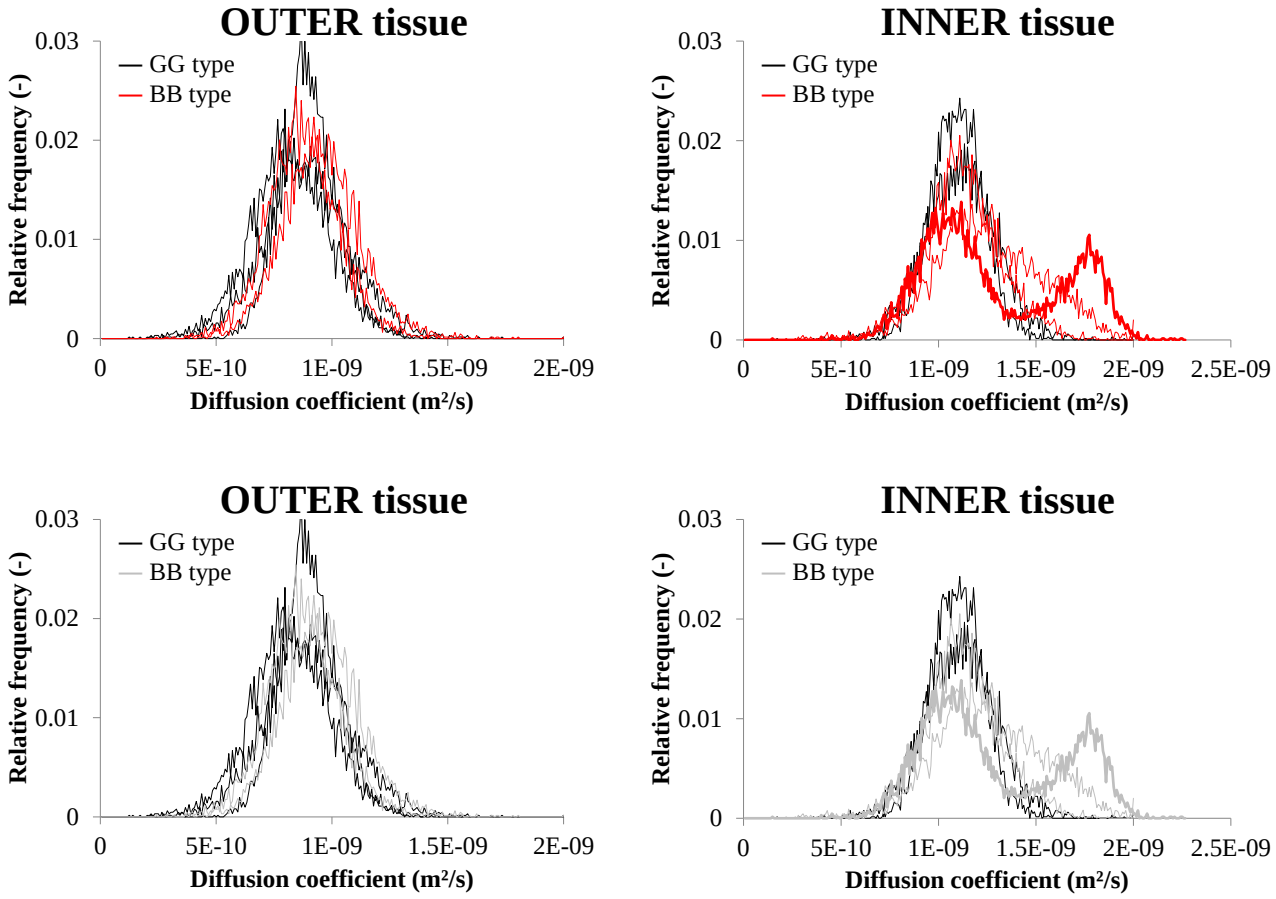

549

550 **Figure 8. Relative frequency distribution of diffusion coefficient (of the ROI) for inner and outer**
551 **tissue: Distinction between apples (types BB and GG) with (red lines) and without (black lines) visual**
552 **internal browning. The bold red line indicates affected inner tissue with a bimodal distribution.**

553

554

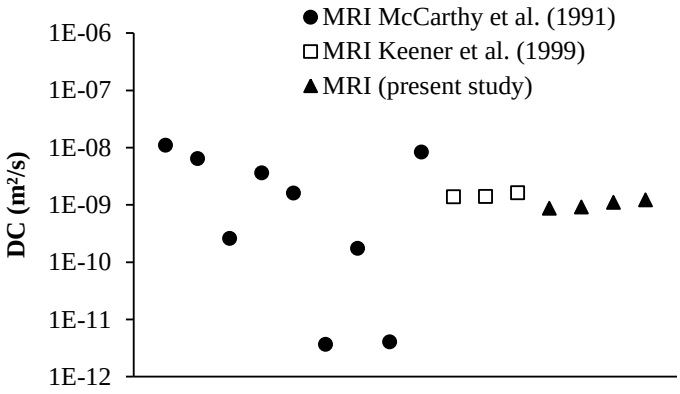

555

556 **Figure 9. Diffusion coefficients of apple (logarithmic scale) as determined by means of MRI**

557 **measurements.**

558

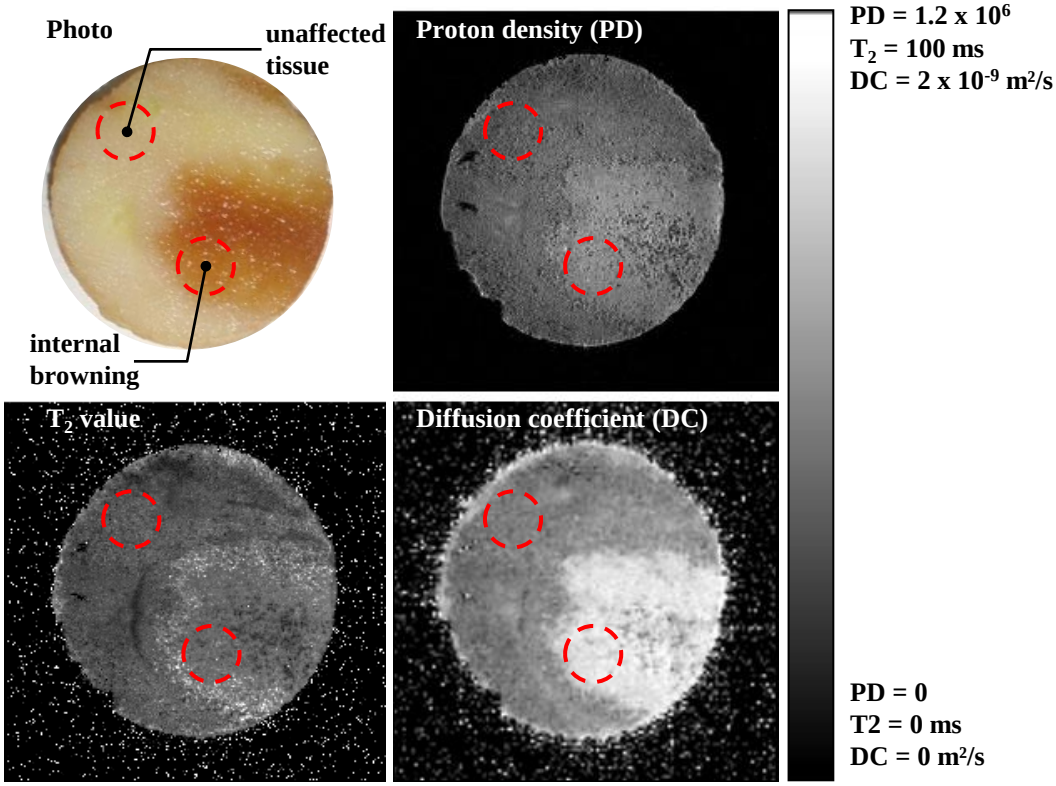
Photo
unaffected tissue
internal browning
Proton density (PD)
T_2 value
Diffusion coefficient (DC)
PD = 1.2 x 10^6
T_2 = 100 ms
DC = 2 x 10^{-9} m²/s
PD = 0
T2 = 0 ms
DC = 0 m²/s

559

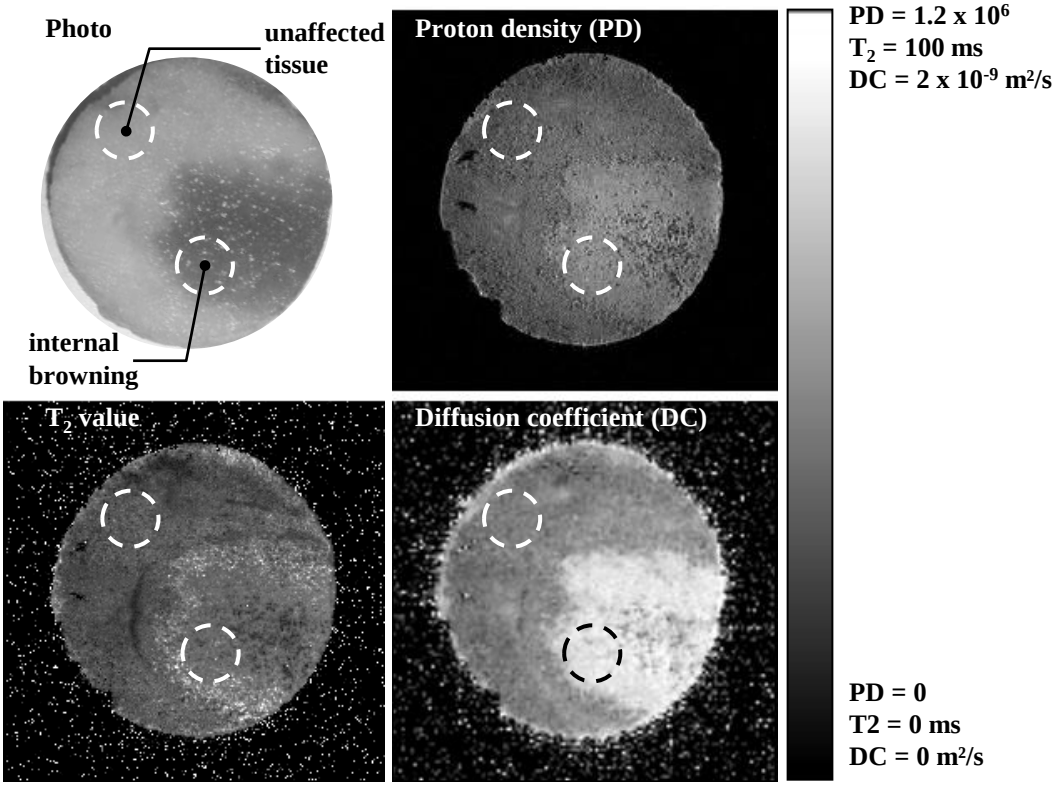
Photo
unaffected tissue
internal browning
Proton density (PD)
T_2 value
Diffusion coefficient (DC)
PD = 1.2 x 10^6
T_2 = 100 ms
DC = 2 x 10^{-9} m²/s
PD = 0
T2 = 0 ms
DC = 0 m²/s

560

561 **Figure 10. A photo, proton density, T_2 value and diffusion coefficient of inner tissue of a typical BB**
562 **type sample with internal browning. The ROI's of the healthy and affected tissue are indicated by the**
563 **circles.**

564

565

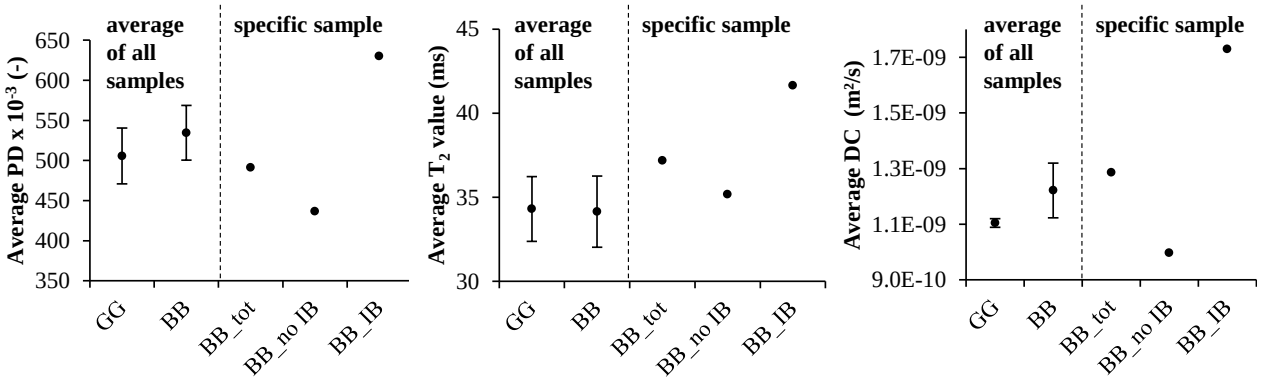

Figure 11. Proton density, T_2 value and diffusion coefficient of inner tissue for all GG samples, all BB samples (mean values of each parameter of all considered samples (see Table 2) and the 95% confidence intervals) and for a specific BB type sample with internal browning (Figure 10), namely for ROI's of the entire sample (BB_tot), healthy (BB_noIB) and affected tissue (BB_IB). These ROI's are indicated in Figure 10.

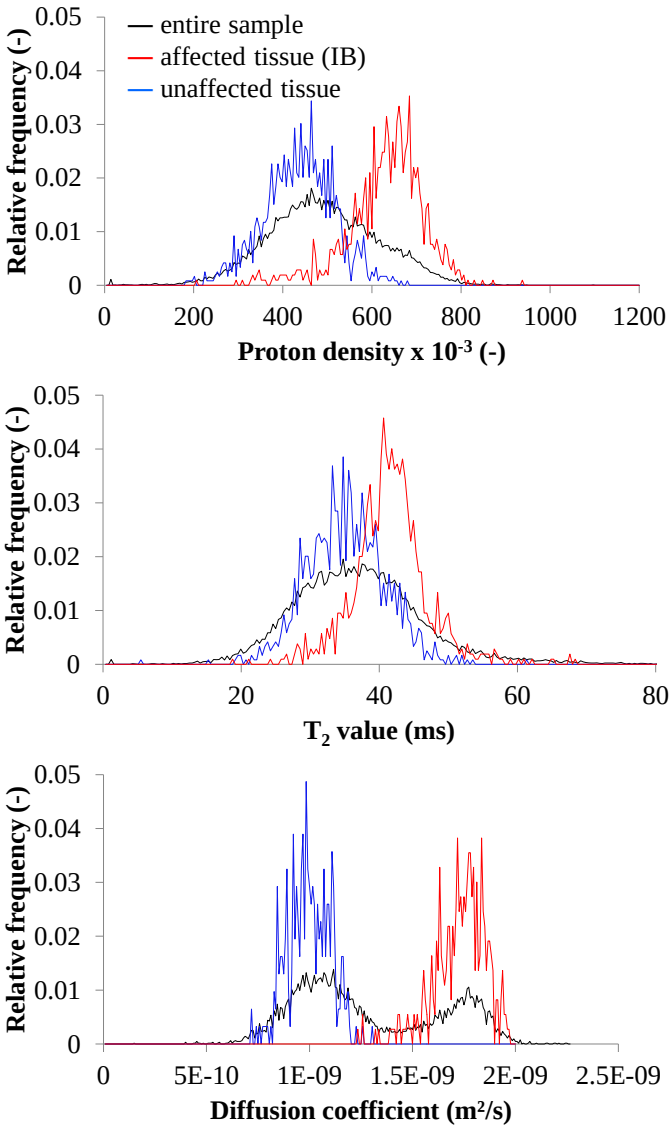
entire sample
affected tissue (IB)
unaffected tissue
Relative frequency (-)
0.05
0.04
0.03
0.02
0.01
0
0
200
400
600
800
1000
1200
Proton density x 10-3 (-)
Relative frequency (-)
0.05
0.04
0.03
0.02
0.01
0
0
20
40
60
80
T2 value (ms)
Relative frequency (-)
0.05
0.04
0.03
0.02
0.01
0
0
5E-10
1E-09
1.5E-09
2E-09
2.5E-09
Diffusion coefficient (m2/s)

574

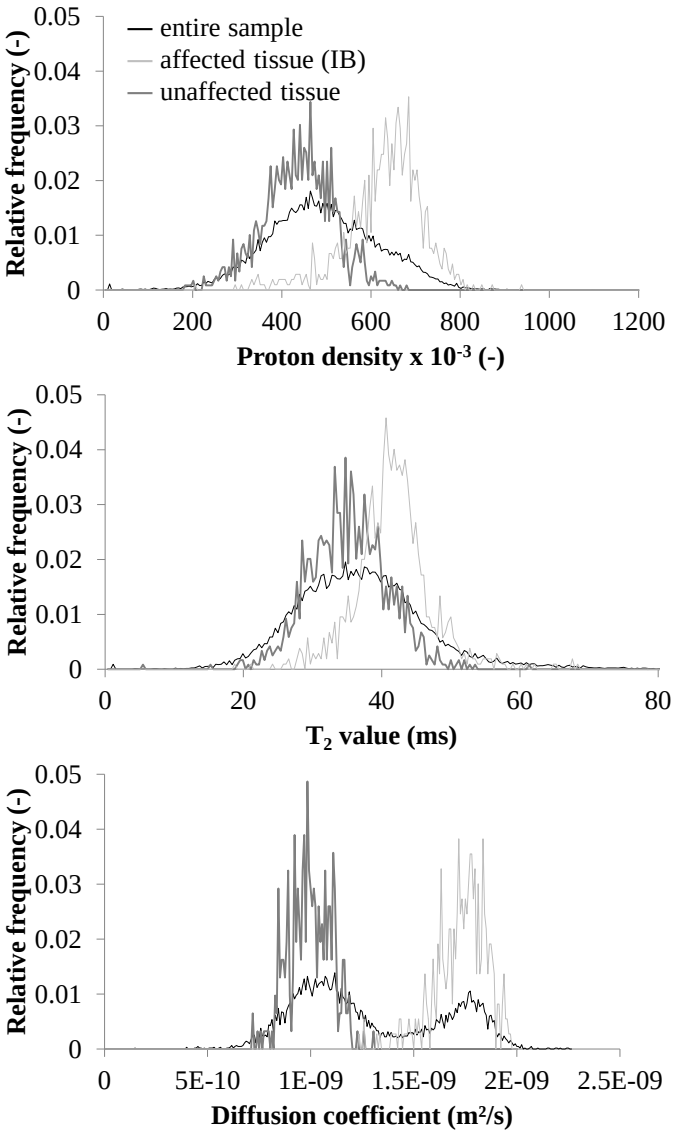

Figure 12. Relative frequency distribution of proton density, T_2 value and diffusion coefficient of inner tissue of a specific BB type sample with internal browning (Figure 10) for ROI's of healthy tissue, affected tissue and the entire sample. The ROI's are indicated in Figure 10.

586 **Tables**

587 **Table 1. Experimental characteristics of MRI measurements on tissue characterisation.**

Method	Multi-spin echo	Diffusion spin echo
Field of view (mm²)	30x30	30x30
Field of view (pixel²)	256x256	128x128
Pixel size (mm)	0.117	0.234
Slice thickness (mm)	0.5	1
Repetition time (T_R) (ms)	3000	2300
Echo time (T_E) (ms)	7-112 (in 16 steps)	13.5
Duration of measurement	12 min	56 min

588

589

590

591 **Table 2. Characteristics of Braeburn apple samples for tissue characterisation with MRI (see section**

592 **2.1 for nomenclature).**

Name	Storage	Fertilisation	Tissue type	Number of measurements		Remarks
				PD & T_2 value	DC	
Measurements November 2010						
0G	-	G	Inner	2	-	No visual IB
			Outer	2	-	No visual IB
0B	-	B	Inner	6	-	No visual IB
			Outer	6	-	No visual IB
Measurements March 2011						
GG	G	G	Inner	4	2	No visual IB
			Outer	5	3	No visual IB
GB	G	B	Inner	2	-	No visual IB
			Outer	2	-	No visual IB
BG	B	G	Inner	2	-	Clear visual IB
			Outer	2	-	No visual IB
BB	B	B	Inner	5	3	Clear visual IB
			Outer	5	2	No visual IB

593